American Mineralogist, Volume 104, pages 659–670, 2019

Zeolite-group minerals in phonolite-hosted deposits of the Kaiserstuhl Volcanic Complex, Germany

Simon Spürgin[1], Tobias Björn Weisenberger[2,*,†], and Marija Marković[3]

[1]Hans G. Hauri KG Mineralstoffwerke, Bergstrasse 114, 79268 Bötzingen, Germany
[2]ÍSOR Iceland GeoSurvey, Grensásvegur 9, 108 Reykjavik, Iceland
[3]Institute for Technology of Nuclear and Other Mineral Raw Materials (ITNMS), Franshe d' Epere 86, 11000 Belgrade, Serbia

Abstract

Subvolcanic phonolite intrusions of the Kaiserstuhl Volcanic Complex (Germany) show variable degrees of alteration. Their secondary mineralogy has been characterized by petrographic textural observations, bulk-rock powder X-ray diffraction, thermogravimetry, differential thermal analysis, and electron probe microanalysis. The alteration assemblage is dominated by various zeolites that occur in fissures, vugs, and as replacement products of primary phases within the phonolite matrix. Phonolites in the eastern Kaiserstuhl were emplaced into a sedimentary sequence and are characterized by high zeolite contents (Endhalden: 48 wt%, Fohberg: 45 wt%) with the temporal sequence: ± thomsonite-Ca ± mesolite – gonnardite – natrolite – analcime. In the western Kaiserstuhl zeolite contents are lower (Kirchberg: 26 wt% or less) and the crystallization sequence is: ± thomsonite-Ca – gonnardite – natrolite – chabazite-Ca. Pseudomorphic replacement textures and barite inclusions in secondary aggregates suggest that zeolites grew at the expense of a sulfate-bearing sodalite-group mineral, i.e., haüyne. Fresh grains of sodalite-haüyne are only found at Kirchberg, whereas the pervasive alteration at Fohberg and Endhalden transformed feldspathoid minerals completely to zeolites.

Zeolites formed in a continuously cooling hydrothermal regime after emplacement and solidification of phonolitic magmas. The common paragenetic sequence corresponds to a decrease in the Ca/Na ratio, as well as an increase in the Si/Al ratio with time. The shift from Ca-Na- to pure Na-zeolites is an expression of closed-system behavior in a water-rich environment at Fohberg and Endhalden, which both intruded an Oligocene pre-volcanic sedimentary unit. The late crystallization of K-bearing chabazite-Ca points to a progressively more open hydrothermal system in the Kirchberg phonolite, which was emplaced in a subaerial volcanic succession and was influenced by K-enriched fluid from leucite-bearing country rock. Therefore, the geological setting and nature of emplacement are important factors that control the degree of zeolitization of intrusive feldspathoid minerals-bearing rocks and whether a zeolite occurrence can be used as mineral deposit.

Keywords: Natrolite, gonnardite, analcime, zeolite, alkaline rocks, phonolite, Kaiserstuhl; Microporous materials: Crystal-chemistry, properties, and utilizations

Introduction

Rock alteration and the formation of secondary mineral assemblages are important processes in the genesis of many types of mineral and ore deposits. In fact, most natural zeolite deposits are the result of decomposition of various primary phases in the presence of aqueous fluids. Differences between zeolite deposits exist regarding modal abundances and the mineralogical complexity of the alteration assemblage, from near-monomineralic to highly diverse, which reflects inherent differences in the reacting source rocks, in fluid accessibility and composition, in thermal regime, and in geologic setting (e.g., de'Gennaro and Langella 1996; Ibrahim and Hall 1996; Langella et al. 2013; Weisenberger et al. 2014; Cappelletti et al. 2015; Atanasova et al. 2017).

Natural zeolites form a large group of tectosilicate minerals characterized by the common feature of an open framework structure enclosing interconnected pores and channels. The three-dimensional framework is built of SiO_4^{4-} and AlO_4^{5-} tetrahedrons in varying proportions but maximum AlO_4^{5-} is limited to unity with SiO_4^{4-} according to Loewenstein's rule (Loewenstein 1954). As a consequence, the aluminosilicate framework contains excess electrons and the walls of zeolitic pores and channels are negatively charged, which allows positively charged ions or bipolar molecules to be fixed in this pore space. Due to the weak bonding strength, these ions and molecules are easily exchanged and replaced by others. The most common extra-framework species in natural zeolites are Na^+, K^+, Ca^{2+}, and H_2O, but several other species, mainly alkali and alkali earth metals and NH^{4+}, are also known to be incorporated. Over 80 naturally occurring zeolite species are defined by Coombs et al. (1997), and over 170 known framework types of natural and synthetic zeolites are illustrated by Baerlocher et al. (2007).

Due to their structure-related physicochemical properties, natural zeolites are an important group of industrial minerals. Technical applications are generally related to their ion-exchange capacity, their reversible dehydration, their regular pore spacing, and their pozzolanic activity, which leads to various applications,

* E-mail: tobias.b.weisenberger@isor.is
† Special collection papers can be found online at http://www.minsocam.org/MSA/AmMin/special-collections.html.

e.g., water and wastewater treatment (Kalló 2001; Al Dwairi et al. 2014; Ibrahim et al. 2016), heavy metal fixation (Napia et al. 2012), soil remediation (Leggo and Ledésert 2001; Leggo et al. 2010), animal feed (Mercurio et al. 2016), agriculture (Faccini et al. 2015), oeonology (Mercurio et al. 2010), the delivery of certain pharmaceuticals (NSAIDs) by surface modified natural zeoites (e.g., Mercurio et al. 2018), the use of zeolite-rich rocks in ancient roman structures (e.g., Jackson et al. 2017; Izzo et al. 2018), and many more.

A major application of natural zeolites is their use in the cement industry as pozzolanic substitute for ordinary Portland cement (OPC) (Mertens et al. 2009; Snellings et al. 2010a, 2012; Özen et al. 2016). Natural pozzolans are silicates or alumina-silicates, e.g., zeolites, which are able to react in an alkaline environment with Ca^{2+} commonly found in cement paste or $Ca(OH)_2$ in a hydrous solution. The reaction products, intergrown hydrated calcium silicates and hydrated calcium aluminates, are comparable to those formed from the hydration of pure OPC (Özen et al. 2016). The pozzolanic reaction is a surface-controlled process based on the hydrolysis of Si-O-Si and Al-O-Si bonds (Snellings et al. 2012). Despite the crystallographic characteristics of the zeolite, a large and not fully recognized number of physicochemical parameters affect their reactivity, including extra-framework cation composition and specific surface of the zeolite material (Mertens et al. 2009; Snellings et al. 2010b), and physicochemical properties of the solution (Snellings et al. 2012). Although not studied systematically yet on pure zeolite phases with controlled conditions, it becomes evident that the pozzolanic reactivity is a general feature of natural zeolites (Mertens et al. 2009; Özen et al. 2016).

Economic deposits of natural zeolites are commonly related to vitreous tuffs from which they formed by decomposition and hydration of volcanic glass. Deposits of this kind are found worldwide in regions of young explosive volcanism (e.g., Cochemé et al. 1996; de'Gennaro and Langella 1996; Ibrahim and Hall 1996; Cappelletti et al. 2015; Özen et al. 2016), Furthermore, there are also examples of zeolite occurrences in intrusive alkaline rocks (Tschernich 1992 and references therein; Schilling et al. 2011; Weisenberger et al. 2014) and their metamorphosed counterparts (Tschernich 1992 and references therein; Chakrabarty et al. 2016; Atanasova et al. 2017).

In the alkaline rock-carbonatite complex of the Kaiserstuhl in southwest Germany, several phonolite intrusions occur that show variable degrees of zeolitization. Despite general similarities in their primary magmatic composition, they exhibit differences in zeolite-dominated alteration, both in quantity (i.e., in their grade) and in mineralogical characteristics, which leads either to economic zeolite deposits or to non-economic zeolite occurrences. By studying the mineralogy and the compositional variations of zeolites in the Kaiserstuhl phonolites, and relating the observations to the geologic setting of each occurrence, we define factors necessary for the formation of economic zeolite deposits in the alkaline intrusive rocks of the Kaiserstuhl Volcanic Complex, which can be adopted for similar occurrences elsewhere.

The Kaiserstuhl Volcanic Complex

The Miocene Kaiserstuhl Volcanic Complex (KVC) is located in the southern part of the Upper Rhine Graben, southwest Germany (Fig. 1), close to the city of Freiburg. The KVC belongs to the Central European Volcanic Province (Wimmenauer 1974) characterized by generally SiO_2-deficient, alkaline intraplate volcanism, formed in the course of the Alpine continent-continent collision (Wedepohl et al. 1994; Wilson and Downes 1991). The KVC is the only larger polygenetic volcanic edifice in the Upper Rhine Graben, but highly silica-undersaturated alkaline dikes and diatremes are common in the graben and along its shoulders. These are represented by the Black Forest, Vosges, and Odins Forest crystalline complexes, and also in their overlying Mesozoic to early Cenozoic sedimentary cover, which is locally preserved inside the graben and along its margins. The magmatic rocks are classified as olivine-melilitites and olivine-nephelinites and are considered unfractionated products of low percentage partial mantle melts (Keller 2001), carrying lherzolitic xenoliths (Keller et al. 1997).

The Kaiserstuhl can be subdivided into two different major geologic units (Fig. 1). (1) The eastern part consists of a sequence of Paleogene sediments (marls, sandstones, and limestones) in a north-south oriented pre-volcanic horst structure. (2) The central-western part consists of volcanic rocks, whereas the central part is formed by a subvolcanic intrusive complex surrounded by effusive and explosive volcanics in the north, west, and south. The Kaiserstuhl most likely had the structure of a complex stratovolcano or a volcanic field with eruptions from various volcanic centers (Keller 2001).

Petrologically the rocks of the KVC form a series from primitive olivine nephelinites toward slightly fractionated basanites, tephrites, and finally phonolites, which were derived from two different parental magmas (Braunger et al. 2018). Carbonatites and carbonate-melilite-bearing silicate rocks ("bergalite") occur in close relationship to nephelinitic diatreme brecciae in the subvolcanic center of the volcanic complex (Keller 2001).

Activity emerged with the eruption of olivine-nephelinites (19.0 ± 1.6 Ma, whole-rock K-Ar age; Baranyi et al. 1976), the deposition of mainly tephritic pyroclastites and lavas (18.2–16.5 Ma) and the emplacement of various subvolcanic intrusions and dikes between 18.4 and 15.3 Ma (Wimmenauer 2003 and references therein). Volcanism ceased with the eruption of the parasitic Limberg-Lützelberg complex at the northwestern margin of the KVC, where a phonolitic tuff was deposited at 16.2 ± 0.2 Ma (Kraml et al. 2006) in a nephelinite-basanite-tephrite-phonolite sequence.

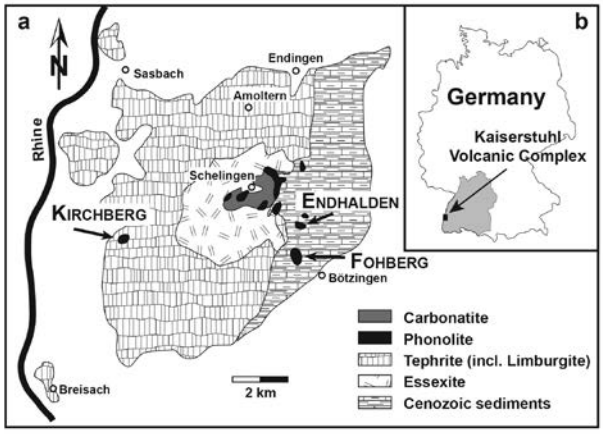

Figure 1. (**a**) Geological map of the Kaiserstuhl Volcanic Complex (KVC), showing the investigated subvolcanic phonolite intrusions, (**b**) map of Germany with the location of the KVC.

Phonolites in the KVC

Phonolites form one of the major petrologic families in the KVC and are subordinate in volume only to the rocks of the tephritic family from which they are derived by fractionation (Braunger et al. 2018). They occur as intrusive subvolcanic stocks and dikes, and as pyroclastic products of explosive volcanic activity. Members of the phonolitic family are recognized by the modal mineralogy: sodic pyroxene (aegirine-augite), alkali feldspar, titanian andradite ("melanite") and sodalite/haüyne. Phonolites from the eastern KVC (Fig. 1) form a distinct subgroup characterized by the presence of wollastonite. These intrusions are apparently arranged on a straight north-south striking line that parallels a major fault located about 1–1.5 km to the west. Larger occurrences of phonolite are found in three different geologic settings in the Kaiserstuhl volcanic edifice (Fig. 1): (1) as intrusions in the subvolcanic center, in close spatial relationship to essexitic and carbonatitic intrusions; (2) as intrusions emplaced into the pre-volcanic Oligocene sediments of the eastern Kaiserstuhl (Fohberg, Endhalden); and (3) as intrusion in subaerial, mainly tephritic pyroclastites and lavas in the western KVC (Kirchberg).

Varieties of phonolite sensu lato occur as small-volume bodies in the KVC. They are represented by decimeter- to meter-thick dikes of tinguaite (feldspar-foid ratio 1:1–1:10), and haüynophyre (Wimmenauer 1962) and leucitophyre (Keller 1964; Spürgin et al. 2008), both with a feldspar-foid ratio of <1:10.

The plutonic facies of the phonolitic family is represented by sodalite syenites (locally more mafic "ledmorite"), and foidolites ("tawite"). They are mineralogically related to phonolites, but with a distinct coarse-grained texture. Occurrences are limited to xenoliths, especially in the Kirchberg phonolite (Czygan 1977), and to the subvolcanic center of the KVC, where ledmorite is recorded as major rock type in a drill core (Wimmenauer 1962, 2003).

Zeolites in the KVC

All silicic lithologies of the KVC were affected by subsequent alteration and zeolitization to variable degrees. Zeolites occur as vesicle-fillings, in fracture assemblages or as fine-grained groundmass replacing components. Processes responsible for alteration include hydrothermal decomposition of primary igneous phases, particularly minerals of the feldspathoid group (Weisenberger et al. 2014), and decay and hydration of volcanic glass either in a hydrothermal or a hydrous low-temperature environment (Eggleton and Keller 1982; Weisenberger and Spürgin 2009). The following zeolite species are reported from the KVC by Weisenberger and Spürgin (2009), Weisenberger et al. (2014), and Marzi and Spürgin (2017): analcime, chabazite-Ca, faujasite-Na, faujasite-Mg, gonnardite, merlinoite, mesolite, natrolite, offretite, phillipsite-K, phillipsite-Ca, and thomsonite-Ca.

Analytical methods

Mineral compositions were determined by electron probe microanalysis (EPMA) at the University of Oulu using a JEOL JXA-8200 electron microprobe. Operating conditions were 15 kV acceleration voltage and 15 nA beam current with counting times of 10 s. Zeolites were analyzed with a defocused beam (20 μm). Sodalite-haüyne was analyzed with a beam diameter of 5 or 10 μm. Na and K were measured first, to minimize the effect of Na and K loss during the determination. Since zeolites lose water when heated, the rock samples and crystals were mounted in epoxy resin to minimize loss of water. Natural and synthetic standards were used for calibration. The charge balance of zeolite formulas is a reliable measure for the quality of the analysis. It correlates with the extent of thermal decomposition of zeolites during microprobe analysis. A useful test is based on the charge balance between the non-framework cations and the amount of tetrahedral Al (Passaglia 1970). Analyses are considered acceptable if the sum E% = 100×[Al-(Na+K)-2(Ca+Sr+Ba)]/[(Na+K)+2(Ca+Sr+Ba)] of the charge of the extra-framework cations (Ca^{2+}, Sr^{2+}, Ba^{2+}, Na^{+}, and K^{+}) is within 7% of the framework charge.

Mineralogical compositions were determined on bulk-rock samples of each phonolite by powder X-ray diffractometry (PXRD) using a Bruker D2 Phaser diffractometer. For this purpose, rock samples of 2–4 kg were crushed, homogenized, and representative subsamples of 50 g were finely ground in a laboratory mill. Scans with Cu$K\alpha$ radiation were recorded in the range $5° < 2\theta < 70°$ with a step width of 0.016° and an integration time of 2 s/step. Full-pattern Rietveld based quantitative phase analyses (QPA) were performed with the Bruker TOPAS software applying a fundamental parameters procedure (Cheary and Coelho 1992; Madsen and Scarlett 2008). Instrumental contributions to the recorded patterns were initially refined on a sample of LaB_6. In the first step of QPA of the phonolite samples, the unit-cell parameters of each phase have been refined to match the observed peak positions. In a second step, the crystallite size and strain functions have been applied to model the peak shape. Further, atomic positions have been allowed to refine in narrow limits, and to limit the number of independently refined parameters, an overall isotropic thermal factor B_{eq} was refined for all atomic sites in all phases. Due to the holocrystalline nature of the phonolites, no amorphous phase content has been refined. Results of QPA are listed in Supplemental[1] Table S1.

Thermogravimetry (TG) and differential thermal analysis (DTA) were performed at the Institute for Technology of Nuclear and Other Mineral Raw Materials (ITNMS). Thermal analysis was performed on a Netzsch STA 409 EP (Selb, Germany). Samples were put in ceramic crucibles and heated (20–1000 °C) in an air atmosphere with a heating rate of 10 °C/min.

Mineral stabilities were obtained using the program SUPCRT92 (Johnson et al. 1992), employing the slop98 database and thermodynamic data from Helgeson et al. (1978) and Neuhoff (2000). Reactions were calculated considering low quartz activity and aluminum conservation in the solid phases.

Results

Mineralogy and petrology of phonolite localities

The three largest phonolite stocks of the KVC, two of them located in the eastern (Fohberg, Endhalden) and one in the western (Kirchberg) Kaiserstuhl (Fig. 1), have been investigated during this study. Their petrographic characteristics are summarized in Table 1. Other known occurrences of intrusive phonolites in the subvolcanic center of the KVC, as well as phonolitic dikes and pyroclastites (Wimmenauer 1962, 2003) have not been considered due to their high degree of weathering in surficial outcrops and their low economic potential regarding minerals of the zeolite group.

Fohberg phonolite. The Fohberg phonolite, 600 × 450 m in aerial size, is the largest phonolite body in the eastern Kaiserstuhl and probably, as outcrop conditions of phonolites in the central KVC allow no correlation and reconstruction, also the largest one in the entire KVC. It intruded a series of Oligocene sediments of the Pechelbronn Formation, mainly marl, limestone, and calcareous sandstone (Wimmenauer 2003), and is cut by a dike of porphyritic essexite.

The petrography of the Fohberg phonolite was investigated by Wimmenauer (1962), and data on the primary and secondary mineralogy is found in Weisenberger et al. (2014). The rock has a slightly porphyritic texture with phenocrysts (≤3 mm) of feldspathoid minerals, aegirine-augite, wollastonite, and andradite in a greenish-gray fine- to medium-grained matrix of sanidine, aegirine-augite, and feldspathoid minerals (Figs. 2a and 2b). Phenocrysts are in general euhedral; however, garnet phenocrysts tend to be subhedral due to possible corrosion. Late magmatic decomposition of mafic phases formed accessory titanite and göt-

zenite, a F- and LREE-bearing Ca-Ti silicate of the rosenbuschite group (Czygan 1973; Albrecht 1981; Weisenberger et al. 2014).

A prominent feature of Fohberg phonolite samples is the complete decomposition of feldspathoid minerals, and the partial replacement of wollastonite. Secondary minerals, which also form large portions of the matrix, include natrolite as sole Na-zeolite end-member, gonnardite, minor thomsonite (both Ca-Na zeolite species), and calcite. Additionally, pectolite and sepiolite occur in minor quantities as alteration products (Weisenberger et al. 2014).

On an outcrop scale, and in contrast to the Endhalden and Kirchberg phonolites, the Fohberg phonolite hosts a network of numerous, mainly steep dipping fractures. These are partially or totally filled with a secondary zeolite-dominated assemblage similar to the altered rock matrix. A temporal succession from Ca-Na species (thomsonite, gonnardite) to pure Na-zeolite (natrolite) is observed (Weisenberger et al. 2014), followed by later phases, e.g., apophyllite, fluorite, and calcite (for a full list see Marzi 1983).

The phonolite at Fohberg is mined by Hans G. Hauri KG Mineralstoffwerke, Bötzingen. Several applications of the rock powder are directly related to its zeolite content and include the use as pozzolan in the cement and concrete industry (Kassautzki 1983), and as cattle feed additive.

Endhalden phonolite. The Endhalden phonolite covers an area of approximately 450 × 250 m and is located about 1 km to the north of the Fohberg phonolite (Fig. 1). It is also in contact to sediments of the Pechelbronn Formation (Wimmenauer

Table 1. General petrographic characteristics of intrusive phonolite stocks in the KVC

Phonolite	Locality	Major primary minerals[a]	Secondary mineral assemblages[a]	Alteration style	Remarks
Endhalden	Bötzingen	Sa, (*FM?*), Aeg, Adr, (Wo)	Ntr, Anl, Gon, Cal, ±Thm, ±Mes, ±clay minerals	vesicles, rock matrix	homogeneous secondary mineralization throughout phonolite body
Fohberg	Bötzingen	(*FM?*), Sa, Aeg, Wo/(Wo), Adr, ±Ttn	Ntr, Gon, Cal, ±Thm, ±Mes	fissures, rock matrix	homogeneous secondary mineralization throughout phonolite body
Kirchberg	Niederrotweil	Sa, Pl, Hyn/(Hyn), Aeg, Adr, Mag, ±Ttn	Cal, Cbz, Clay minerals Thm, Gon Ntr, Gon, Thm Cal, Cbz, clay minerals Cbz, clay minerals clay minerals	fissures (partially), rock matrix (partially)	various assemblages; heterogeneous secondary mineralization throughout phonolite body

[a] Mineral abbreviations after Whitney and Evans (2010), except Gon = gonnardite; *FM?* = unidentified feldspathoid mineral (most likely a member of the sodalite group, see text). Aeg refers to aegirine-augite solid solution. Mineral abundances are noted on a qualitative basis. Mineral names in parentheses: primary mineral decomposed and only recognized due to shape of pseudomorphic aggregates.

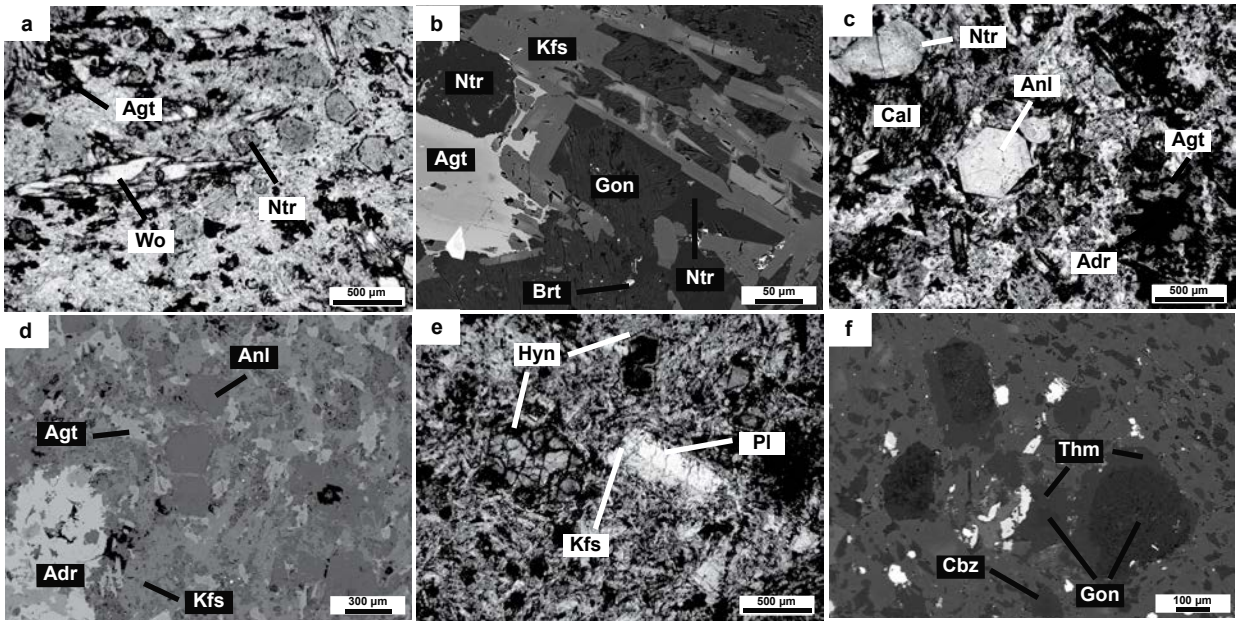

Figure 2. Representative thin section microphotographs and BSE images of phonolites from the KVC. (**a** and **b**) Wollastonite-bearing, slightly porphyritic phonolite from Fohberg. The phonolite shows pseudomorphic replacement of feldspathoid minerals by various zeolites. Barite is present as small inclusions in zeolite aggregates. (**c** and **d**) Endhalden phonolite with similar igneous textures as Fohberg phonolite. In addition, analcime is present as secondary mineral. (**e** and **f**) Kirchberg phonolite showing primary fresh feldspathoid minerals, as well as an example of a zeolite alteration sequence. Mineral abbreviations: Adr = andradite, Agt = aegirine-augite, Anl = analcime, Brt = barite, Cal = calcite, Cbz = chabazite, Gon = gonnardite, Hyn = haüyne, Kfs = alkali feldspar, Pl = plagioclase, Thm = thomsonite, Wo = wollastonite.

2003), but no physical connection between the Endhalden and the Fohberg phonolite bodies is exposed or known, which can indicate their co-genetic formation.

The shape and structural position of the Endhalden phonolite is not clarified yet. Shallow vertical drill cores indicate that the Endhalden phonolite is emplaced on top of a clay-dominated sedimentary unit. It may represent a shallow intrusive body like a sill, small laccolith, or cryptodome, or a subaerial feature like an erosional remnant of a thick lava flow or extrusive dome.

Petrographically the Endhalden phonolite closely resembles the Fohberg phonolite. It is weakly porphyritic to various degrees, with a similar set of phenocrysts (feldspathoid minerals, sanidine, aegirine-augite, wollastonite, andradite) within a medium- to fine-grained groundmass of sanidine, aegirine-augite and feldspathoid minerals (Figs. 2c and 2d). K-feldspar and feldspathoid minerals often show a poikilitic texture hosting very-fine-grained aegirine-augite inclusions.

As in the Fohberg phonolite, all primary igneous feldspathoid minerals are completely replaced by zeolites and calcite. Wollastonite is always decomposed. In contrast to the Fohberg alteration assemblage, analcime occurs as a second Na end-member zeolite together with natrolite, and minor mesolite is found as an additional Ca-Na species besides gonnardite and thomsonite.

The Endhalden phonolite is unique as it exhibits only very limited hydrothermal fracturing, but is rich in vesicles, up to 1.5 cm in size, which often contain euhedral zeolite fillings (analcime and/or natrolite), particularly in the upper part of the phonolite body.

Kirchberg phonolite. With an extent of 430 × 200 m, the Kirchberg phonolite is the only stock-like body intruding pyroclastites and lavas of the subaerial volcanic facies of the western KVC. It is in intrusive contact to tephritic ash tuffs to tuff breccia, and to carbonatitic ash- to lapilli tuffs. Rafts of country rock occur in the outermost 10–20 m of the phonolite stock. Along the contact zone to subaerial country rock, the gray-brown colored phonolite grades into light gray marginal facies.

The petrography of the Kirchberg phonolite was reported by Wimmenauer (1962). Despite general similarities, it shows characteristic differences compared to the Fohberg and Endhalden phonolites. The porphyritic texture is less developed, dominated by groundmass phases, resulting in a fine- to medium-grained texture. Apart from the characteristic set of phases for phonolites in the KVC (haüyne, sanidine, aegirine-augite, andradite), the Kirchberg phonolite contains phenocrysts of euhedral to corroded plagioclase, which is often overgrown by K-feldspar. In contrast to the Fohberg and Endhalden phonolites, the Kirchberg phonolite contains no wollastonite, but fresh grains of haüyne and sodalite (Wimmenauer 1962; Spürgin et al. 2014), pigmented by hematite, are common (Fig. 2e).

Although the Kirchberg phonolite is also affected by zeolite-forming alteration (Fig. 2f), the intensity is very heterogeneous and less pronounced than in the phonolites from the eastern KVC. The secondary assemblage contains natrolite, thomsonite, gonnardite, and chabazite-Ca, and minor amounts of clay minerals. Additional secondary minerals, generally found in fractures, are listed by Wimmenauer (1962) and include calcite, apophyllite, gypsum, and others.

Quantitative mineralogy

The results of bulk-rock PXRD and QPA (Supplemental[1] Table S1) show the mineralogical composition of the three phonolites. The Fohberg and Endhalden phonolites show the highest zeolite contents with proportions X_{Zeo} = Zeo/(Zeo+Fsp) in the range of 0.3–0.6. Gonnardite is the major zeolite species in one sample (Fohberg_7) and accounts to approximately 10–20% of the total sodic zeolite content [natrolite, gonnardite, analcime; X_{Gon} = Gon/(Ntr+Gon+Anl) = 0.1–0.2] in the other samples. Analcime is restricted to the Endhalden phonolite, where also the calcite content is notably higher. Low total zeolite contents in combination with the presence of clay minerals in sample Endhalden_5 are an expression of surficial weathering in the outcrop.

In contrast, the Kirchberg phonolite contains a higher amount of alkali feldspar and, in one case (Kirchberg_4) also intermediate plagioclase as well as less clinopyroxene and no wollastonite. Zeolite contents are highly variable. The mineralogy of sample Kirchberg_3 resembles those from Endhalden except for a high gonnardite content that is reflected by X_{Gon} = 0.4, but in other samples only minor quantities of zeolites (gonnardite and chabazite) could be identified. Sodalite-haüyne, which is known to occur at Kirchberg, was detected by PXRD in two samples but could not readily be quantified. The content of sodalite-haüyne is believed to be underestimated and should be in the order of more than 10%, according to thin section observations. Wimmenauer (1962) reports an average of 61 vol% feldspar and 28 vol% sodalite-haüyne, including products of its decomposition.

Zeolite chemistry and paragenesis

Zeolite phases were identified and characterized using PXRD and EPMA, except mesolite because it was only detected by EPMA due to its rarity and very small grain size. The chemical composition of zeolite species is presented in Supplemental[1] Table S2 and Figure 3. Considering the ternary system Ca-Na-K the following succession is observed with decreasing Ca concentrations: thomsonite-gonnardite-natrolite-analcime. Textural relationships in alteration assemblages indicate that this chemical trend defines a common temporal succession. In addition, chabazite is observed only in the Kirchberg phonolite, where it occurs as the latest generated zeolite.

Gonnardite. Gonnardite is generally less abundant than natrolite, but may reach similar concentrations in some parts of the Fohberg phonolite. It is an early crystallizing secondary phase of the rock matrix, and forms an early phase of fissure assemblages, where it nucleates at the fissure walls and is overgrown by natrolite. Gonnardite compositions from Fohberg (Weisenberger et al. 2014) and Endhalden form a continuous trend from Na-Al- (T_{Si} = 0.55) toward Ca-Si-rich compositions (T_{Si} = 0.59), whereas Kirchberg gonnadite is chemically distinct due to considerably higher Na concentrations at moderate T_{Si} (0.56). Gonnardite analyses from the Fohberg and Endhalden localities yield Sr concentrations up to 0.39 atoms per formula unit (apfu). It cannot be excluded that this elevated Sr concentration may result from submicroscopic inclusions of another Sr-bearing phase (e.g., thomsonite).

Thomsonite-Ca. Thomsonite-Ca is occasionally present as an early-formed secondary phase in all three phonolites (Fig. 2f). It has the lowest Si/Al ratio (T_{Si} = 0.52) of all zeolites found in the KVC (Weisenberger and Spürgin 2009), and at Fohberg and

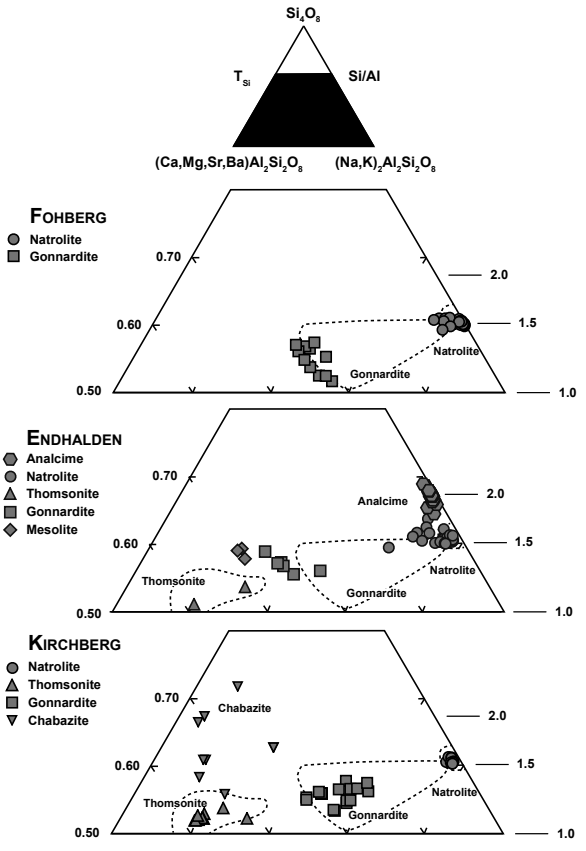

FIGURE 3. Chemical characterization of zeolites from phonolites of the KVC, showing variations in extra-framework cations and T_{Si} = Si/Al variations in the Si-R^{2+}-R^{+} plot. The dashed areas represent compositional variation for particular zeolite species (adapted from Deer et al. 2004).

Endhalden, it is the most Ca-rich zeolite species. Thomsonite-Ca from Endhalden is Sr-rich with a maximum content of 3.16 Sr apfu (equal to 26% of extra-framework cations).

Mesolite. Mesolite is an infrequent Ca-Na-zeolite in the Fohberg and Endhalden phonolites. Chemical analyses of the Endhalden mesolite are close to the ideal stochiometric composition (T_{Si} = 0.59). Weisenberger et al. (2014) report thin, elongate mesolite inclusions of approximately 1 × 50 μm with a growth orientation along the c-axis in large natrolite grains from the Fohberg phonolite.

Natrolite. Natrolite is present in all KVC phonolites, and it is the dominant zeolite species in the Fohberg and the Endhalden phonolites. It forms centimeter-size, transparent euhedral needles in fissures of Fohberg and Kirchberg, and smaller crystals in vugs of Endhalden. Furthermore, natrolite is a major phase in the Fohberg groundmass, and to a lesser degree in the Endhalden phonolite. It is preceded by gonnardite and thomsonite-Ca, and overgrown by analcime, calcite, and other minerals of the secondary assemblage (Marzi 1983), where present. Especially at the Endhalden locality, natrolite may contain distinct amounts of Ca (up to 0.47 apfu based on 80 framework O atoms), which is also a common feature seen in analyses from other occurrences (Ibrahim 2004; Çiftçi et al. 2008; Kónya and Szakáll 2011). Concentrations of all other exchangeable cations are negligible, and T_{Si} shows only limited variations with an average value of 0.61.

Analcime. Besides natrolite, analcime is the characteristic zeolite species in the Endhalden phonolite. It is part of the rock matrix and also forms clear, euhedral crystals several millimeters in size filling open vugs. Petrographic observations indicate that analcime always postdates natrolite, and it may be overgrown by anhedral masses of calcite. Most analcime analyses show near-end-member composition, in a few cases with minor incorporation of K-component. It is the most Si-rich (T_{Si} = 0.67) zeolite species in the Endhalden phonolite.

Chabazite-Ca. Chabazite-Ca is sporadically found in the groundmass of the Kirchberg phonolite (Supplemental[1] Table S2 and Fig. 2f). It shows a wide compositional range in Si-R^{2+}-R^{+} space and is the only zeolite species in KVC phonolites that incorporates a significant K component. It has a highly variable Si/Al-ratio ($0.56 < T_{Si} < 0.72$) and is the most Si-rich zeolite at Kirchberg (Fig. 3).

Other secondary minerals. Calcite is found in variable proportions as a secondary alteration product in all phonolites. In contrast to the Fohberg and Kirchberg phonolites, where calcite appears as a minor alteration phase, the Endhalden phonolite exhibits larger quantities of calcite (Supplemental[1] Table S2). Chemical analyses reported by Weisenberger et al. (2014) from Fohberg indicate pure calcium carbonate with only very little incorporation of Mn (0.02 apfu) and Fe (0.01 apfu).

Minor quantities of clay minerals are found within the phonolite intrusions. During electron probe microanalysis a platy mineral phase has been observed filling interstitial pores in the Kirchberg phonolite. Silica and Al are the dominant cations with a Si/Al ratio of about 1 and variable trace amounts of Fe, Mg, and Ca. A subsequent X-ray diffraction analysis of the sample indicated that the most likely phase is halloysite [$Al_2Si_2O_5(OH)_4$]. Sepiolite and pectolite have been described by Weisenberger et al. (2014) in the Fohberg phonolite as minor alteration products.

Various other secondary minerals, which generally postdate the zeolite assemblages of fissures in the Fohberg and Kirchberg phonolites, are reported by Wimmenauer (1962) and Marzi (1983).

Thermal behavior

The thermal behavior of bulk-rock samples was determined by TG-DTA, the results are shown in Figure 4. Samples from Endhalden and Fohberg show pronounced weight loss steps in the temperature intervals of 300–380 °C and ca. 700–800 °C, which correspond to the single-step dehydration of natrolite and the calcination of calcite, respectively (van Reeuwijk 1972; Deer et al. 2004; Rodriguez-Navarro et al. 2009). Although natrolite is the thermally most active mineralogical phase, contributions of other phases, like other minor zeolite species and clay minerals, cannot be excluded. The reactions of natrolite and calcite are reflected by strong endothermal peaks in DTA plots (Fig. 4). Furthermore, a steady weight loss in the region below 300 °C, and additional minor endothermal signals slightly below 100 °C, at 200–250 °C and at 460–480 °C, is evident in sample Fohberg_7. These are related to the multistep dehydration and final structure collapse of abundant gonnardite in this sample (van Reeuwijk 1972). The effect of analcime dehydration, which contributes to a general weight loss in the region from 250 to 450 °C (Harada and Nagashima 1972),

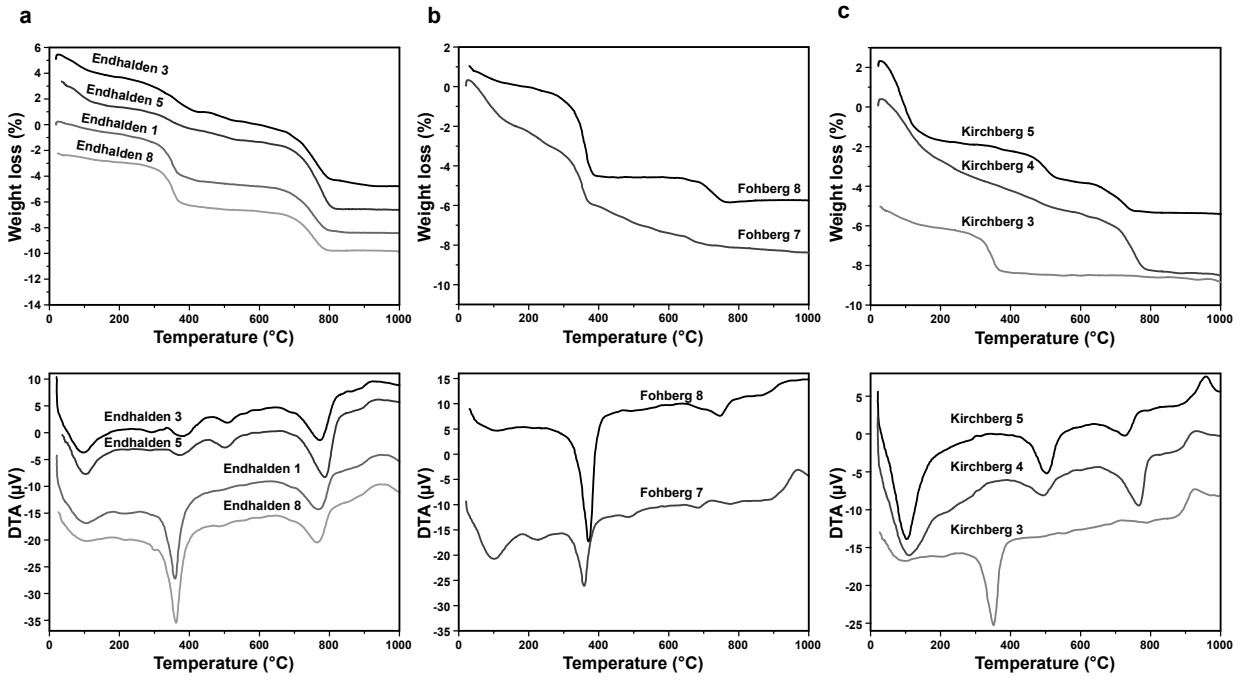

Figure 4. Thermal behavior of phonolites (**a**) Endhalden, (**b**) Fohberg, and (**c**) Kirchberg. Major weight loss in TG plots (upper diagrams) and endothermal peaks in DTA plots (lower diagrams) correspond to H_2O loss of zeolites and CO_2 loss of calcite.

remains largely unresolved in the Endhalden samples. It is only evident by a very minute endothermal signal at 300 °C, on the low-temperature flank of the large natrolite peak.

The Kirchberg phonolite shows the largest variations with individual patterns for each sample. Sample Kirchberg_3 is dominated by natrolite dehydration and shows no further reactions except a steady weight loss below 300 °C, whereas the reaction curves of samples Kirchberg_4 and Kirchberg_5 are combined patterns of zeolite dehydration, clay dehydration and calcination of calcite in variable proportions.

Discussion

Zeolite precursor phase

All phonolites investigated in this study are holocrystalline subvolcanic intrusive rocks. No evidence is found for the presence, or the former presence, of volcanic glass, which is an important zeolite precursor phase in many zeolite deposits elsewhere formed from vitreous volcanic tuffs. However, the presence of feldspathoid minerals as members of the pyrogenic assemblages is evident in all three phonolites. They occur as dominant phenocryst phases, ranging in diameter between 0.1 and 1 mm (Figs. 2a and 2e), and as a fine-grained matrix phase. Pseudomorphic aggregates of replaced feldspathoids in all three phonolites commonly show a dark or orange rim, which may be caused by submicroscopic inclusion of Fe-phases.

Unaltered phenocrysts of feldspathoids are only found in the Kirchberg phonolite. The chemical composition is shown in Supplemental[1] Table S3 and Figure 5. Sodalite-group mineral classification based on the Ca-Na-K system indicates that this feldspathoid mineral is haüyne. Classification by volatiles implies that the SO_3 concentrations are underestimated by electron probe microanalysis, which may also explain the low totals (Supplemental[1] Table S3). However, the Kirchberg phonolite shows a heterogeneous alteration and haüyne may be replaced by secondary minerals like zeolites (chabazite, gonnardite, natrolite, and thomsonite) and calcite.

Phenocrysts and matrix feldspathoid minerals in the Fohberg and Endhalden phonolites are totally altered to aggregates of fibrous spherulitic zeolites (including analcime, natrolite, thomsonite, and gonnardite), calcite, and barite, leaving pseudomorphs with characteristic hexagonal and rhombic dodecahedral shape and few rectangular cross sections (Fig. 2a). The common association of barite grains with these pseudomorphic aggregates (Fig. 2b), in combination with the geometry of the aggregates, points to an S/SO_4-bearing sodalite group mineral as precursor phase, e.g., haüyne or nosean. The following reaction shows the breakdown of a hypothetical barium component in haüyne to natrolite and barite:

$$Na_6Ba_2Al_6Si_6O_{24}(SO_4)_2\ (Hyn) + 3SiO_{2,aq} + 6H_2O \rightarrow 3Na_2Al_2Si_3O_{10}\cdot 2H_2O\ (Ntr) + 2BaSO_4\ (Brt)$$

However, no unaltered relics of feldspathoid minerals have been identified in the Fohberg (Weisenberger et al. 2014) and Endhalden phonolites so far. Highly Ba-enriched beforsite (Keller 2001), which is found as late-stage centimeter-sized veins within the carbonatite complex of the central KVC (Fig. 1), may also account as a source of Ba. However, because it occurs in a spatially and geologically different context and is volumetrically insignificant, it is assumed that Ba is locally derived and precipitated as barite in the phonolite alteration assemblages.

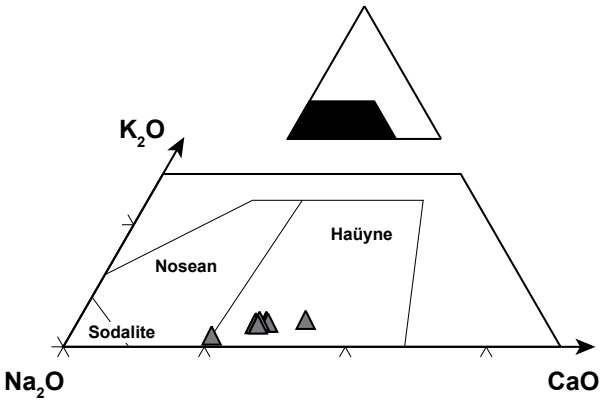

Figure 5. Chemical composition and classification of sodalite-group minerals from the Kirchberg phonolite.

Hydrothermal alteration

Degree of alteration. As described by Weisenberger et al. (2014) for the Fohberg phonolite, the conversion of an essentially anhydrous primary mineralogy to a zeolite-dominated and therefore water-rich assemblage and the syn- to post-deformation mineralization and healing of brittle fractures is likely a scenario of hydrothermal overprinting of the Fohberg phonolite body during post-magmatic cooling and late-stage circulation of meteoric fluids. Although fracturing and fracture mineralization within the Endhalden and Kichberg phonolites are limited, a similar scenario of sub-solidus alteration during post-magmatic cooling and late-stage circulation of meteoric fluids is applicable.

In general, the secondary mineralogy is very similar in all three phonolites, showing the same general trend from early formed Ca-Na zeolites toward Na-dominated zeolites during subsequent alteration. Nevertheless, alteration shows differences that are controlled by fluid-rock interaction and the physicochemical properties of the fluid rather than by the primary chemical and mineralogical composition of the host rock.

Sub-solidus alteration is marked by the breakdown of haüyne as the dominant feldspathoid mineral. In addition, partial wollastonite breakdown occurs in the Fohberg (Weisenberger et al. 2014) and Endhalden phonolites, as wollastonite is only present there. Plagioclase, which only occurs in the Kirchberg phonolite, shows no sign of alteration and gives evidence for the limited overall alteration of the Kirchberg phonolite. The hydrothermal alteration within the two eastern phonolites (Fohberg and Endhalden) is pervasive; secondary minerals replace all primary feldspathoid minerals. The intensity of wollastonite breakdown in the Fohberg phonolite is very heterogeneous from fresh grains toward fully decomposed ones, in contrast to the Endhalden phonolite where wollastonite is completely replaced. The degree of alteration within the Kirchberg phonolite differs significantly as it still contains primary haüyne, with only limited zeolite- and clay-forming alteration. The change in the degree of alteration between the Kirchberg phonolite and the two phonolites within the eastern part of the KVC is directly related to differences in the country rocks in which the phonolites have been intruded (Fig. 6). The Kirchberg phonolite is emplaced into a pile of volcanic rocks, whereas the two eastern phonolites are situated within a pre-volcanic sedimentary sequence of lime- and mudstones (Wimmenauer 2003). A stable isotope study of secondary calcite from the Fohberg phonolite (Weisenberger et al. 2014) suggests that fluids were derived from the surrounding sedimentary succession. In contrast, $^{87}Sr/^{86}Sr$-isotope studies (Wimmenauer 2010; Weisenberger et al. 2014) suggest that Ca, as a major constituent in secondary minerals of the phonolites, is locally derived from the magmatic parent rock. This indicates that the lime- and

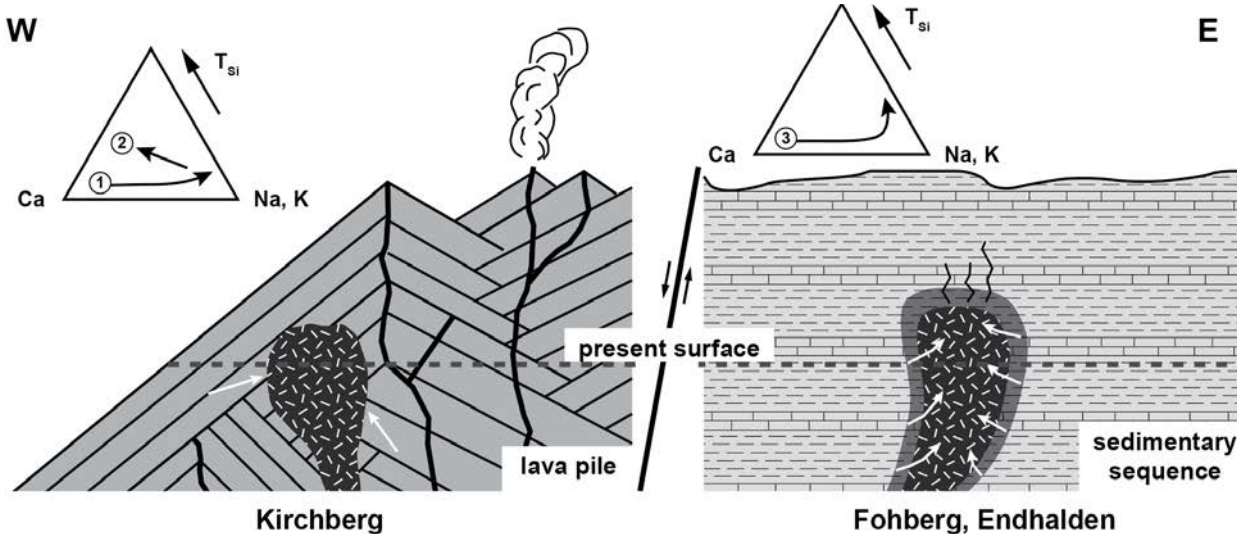

Figure 6. Geological sketch section showing the setting of phonolites in the western (left) and eastern (right) Kaiserstuhl. The dashed line represents the present erosional level. White arrows indicate fluid influx. Triangular diagrams show the temporal succession of zeolite formation (for full labeling see Fig. 3). The Kirchberg phonolite is a shallow intrusion into relatively dry subaerial lavas and pyroclastites. After an initial closed-system evolution (1) limited influx of K-rich water from leucite-tephritic country rock led to the formation of chabazite (2). The Fohberg and Endhalden phonolites were emplaced into a pre-volcanic sedimentary sequence and experienced an influx of formation water during cooling, which established a hydrothermal system and continuous, pervasive closed-system zeolite formation (3).

mudstones have been dehydrated during the emplacement of the phonolites, and aquifers in these lithologies have been tapped and drained into the cooling phonolite intrusions. This is supported by the contact metamorphic overprint of the underlying mudstone of the Endhalden phonolite, in which a dehydration front is developed (Spürgin et al. 2014). The Kirchberg phonolite, in contrast, intruded a sequence of subaerial lavas and pyroclastites. Although the volcanic pile shows evidence of alteration due to the emplacement of the Kirchberg phonolite, the thermal alteration of nearly anhydrous volcanic rocks does not have the potential to deliver volatiles that could cause a pervasive alteration of the Kirchberg phonolite.

It is noted by previous studies on phonolite tuff deposits that fluid accessibility controls the alteration of volcanic products and the formation of zeolites (e.g., de'Gennaro et al. 2000; Bernhard and Barth-Wirsching 2002). However, within some pyroclastic deposits the formation of zeolites is related to groundwater flow (de'Gennaro et al. 2000; Hay and Sheppard 2001; Bernhard and Barth-Wirsching 2002). In contrast, the alteration within intrusions is more related to the presence and the accessibility of fluids, and open system behavior during sub-solidus cooling and deviation from auto-metasomatic conditions. Thereby, for the two eastern phonolites, the thermal regimes are assumed to represent near auto-metasomatic conditions, with externally derived fluids from the surrounding sediments infiltrating into the sub-solidus cooling intrusions, as it was postulated for the Fohberg phonolite by Weisenberger et al. (2014). In contrast, the Kirchberg phonolite indicates open system behavior, as a result of a thermal and maybe a chemical gradient within the hydrothermal system. The open system behavior of the Kirchberg phonolite is further supported by the very limited amount of natrolite, indicating only a limited fluid change during hydrothermal evolution, most likely caused due to local disequilibrium, even though a Na depletion is observed within the Ca-Na zeolites. Furthermore, all analyzed samples from the Kirchberg phonolite yield different alteration assemblages. During experimental studies, Barth-Wirsching and Höller (1989) noted that the effect of solution chemistry and reaction time is greater in open systems, whereas the influence of the starting material may entirely be eliminated by material transport possible in an open system. This can explain the variability in alteration of the Kirchberg samples. In contrast, the two eastern phonolite intrusions exhibit large quantities of both Ca-Na and Na zeolites in a temporal succession; these species are present throughout all samples with only minor variations, indicating a closed system behavior (Hay and Sheppard 2001).

Fluid evolution. Fluid evolution can be illustrated in the systems Al_2O_3–SiO_2–CaO–Na_2O–H_2O (Fig. 7) and Al_2O_3–SiO_2–Na_2O–H_2O (Fig. 8) and in terms of mineral stability as function of aqueous species (Ca^{2+}, Na^+, $SiO_{2,aq}$, H_2O) at low temperature and pressure.

Figure 7 illustrates the change in fluid composition during the hydrothermal replacement as a function of aqueous cation (Ca^{2+}, Na^+) to hydrogen ion activity ratios at temperatures of 50 and 100 °C, and pressure of 10 MPa. The overall topology of stability fields does not change with small variations of pressure; therefore, the uncertainty of the emplacement depth can be ignored. Due to a lack of reliable thermodynamic data for gonnardite, mesolite appears instead as intermediate Ca-Na zeolite (Rogers et al. 2006). The chemical evolution of fluids during zeolite formation can be expressed by the observed sequence marked by Ca-Na zeolite species and natrolite (Fig. 7). At higher SiO_2 activity analcime appears instead of natrolite.

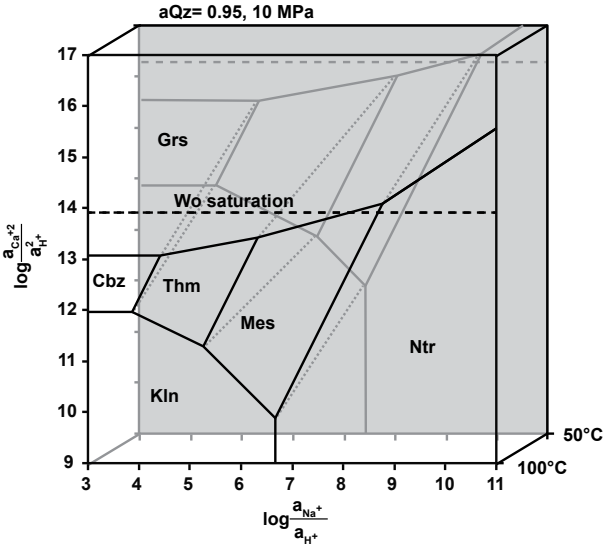

FIGURE 7. Calculated mineral stability diagram between 50 and 100 °C at a constant pressure of 10 MPa as a function of cation activity ratios in the Al_2O_3–Na_2O–CaO–SiO_2–H_2O system. The diagram assumes aluminum balance and quartz undersaturation (a_{Qz} = 0.95) and a_{H_2O} = 1. Mineral abbreviations: Cbz = chabazite, Grs = grossular, Kln = kaolinite, Mes = mesolite, Ntr = natrolite, Thm = thomsonite, Wo = wollastonite.

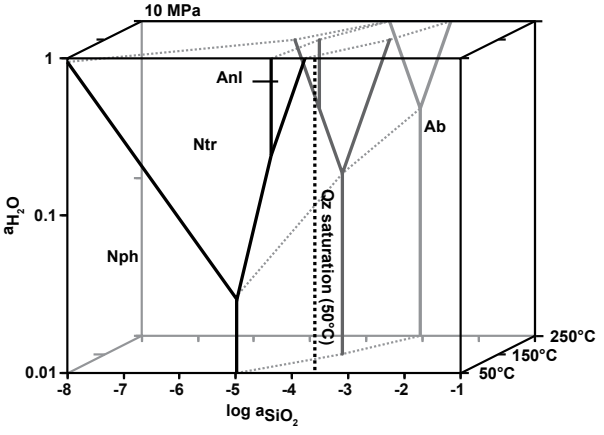

FIGURE 8. Quantitative a_{SiO_2}-a_{H_2O} diagrams for selected Na–Al silicates at constant pressure (10 MPa) within the temperature range from 50 to 250 °C. Dashed lines represent the lower limits of quartz saturation at 50 °C. Mineral abbreviations: Ab = albite, Anl = analcime, Ne = nepheline, Ntr = natrolite, Qz = quartz.

Similar sequences are observed in basaltic lavas in the Disko-Nuussuaq region, West Greenland (Neuhoff et al. 2006; Rogers et al. 2006) and in the Kahrizak area, Iran (Kousehlar et al. 2012), and are interpreted to have formed in a chemically distinct alteration style that reflects the Ca-poor and Si-rich primary compositions of these lavas in contrast to provinces with more evolved basaltic rocks, like in Iceland (Neuhoff et

al. 1999; Weisenberger and Selbekk 2009) or East Greenland (Neuhoff et al. 2006).

The alteration mineralogy within the three phonolite bodies shows a general compositional shift from clay minerals (halloysite) to Ca-Na zeolite species (gonnardite, thomsonite, mesolite) and further to the Na end-members natrolite and analcime. Ca-Na zeolites, in particular thomsonite and gonnardite can locally incorporate higher Sr concentrations (Supplemental[1] Table S2). However, no systematic Sr distribution is observed, and the incorporation of Sr may be caused by local Sr inhomogeneities either within the primary phases or within fluids. The paragenetic sequence corresponds to a decrease in the Ca/Na ratio, as well as an increase in the Si/Al ratio with time (Fig. 3). Nevertheless, a single phonolite body does not cover the entire mineral sequence. The general sequence is characterized by the appearance of thomsonite and gonnardite and followed by natrolite. Fluid-rock interaction results in the evolution of Ca-Na zeolites with a general shift to Na-dominated zeolites.

The Kirchberg sequence is characterized by the stability of clay and chabazite. The crystal chemistry of chabazite (Fig. 3) is unique as it is the only zeolite species found in this study that is able to accommodate a significant amount of potassium. The occurrence of late potassium-bearing chabazite, which postdates the Ca-Na zeolite succession, suggests the infiltration of meteoric water with high calcium and potassium concentration whose composition became a significant component in total fluid composition at a certain time. This water originated in and was in equilibrium with the leucite-tephritic country rock, where leucite served as a source for potassium. A potassium source in the phonolite itself can be excluded due to the fresh appearance of K-bearing phases, i.e., feldspars.

The Fohberg and Endhalden phonolites are both characterized by the occurrence of large quantities of Ca-Na and Na species, showing the general trend from Ca-Na to Na-end-member zeolite species. Although the bulk-rock composition and primary mineral chemistry of the Fohberg and Endhalden phonolites are nearly identical (Spürgin et al. 2014) the alteration mineralogy yields significant differences by the appearance of analcime in the Endhalden phonolite. This indicates that the hydrothermal systems evolved under different conditions during their final stages. Nevertheless, both hydrothermal systems are characterized by a general closed system behavior, whereas the change in mineralogy reflects continuing fluid-rock interaction (Fig. 8) characterized by Ca-depletion and Na-enrichment, as well as an increase in Si/Al of the zeolite species with time (Fig. 3).

Figure 8 illustrates the change in fluid composition during hydrothermal replacement as a function of aqueous silica activity and H_2O, respectively, and allows an estimation at fixed pressure and temperature. The calculated quartz saturation plots at higher silica activities than the observed phase equilibrium that buffers the activities of water and silica. This is in agreement with the absence of quartz in the alteration assemblages. At a sub-solidus temperature of 250 °C, nepheline and albite buffer log $a_{SiO_{2,aq}}$ to equilibrium values of –4 to –3 and at $a_{H_2O} = 0.5$, analcime is the only stable zeolite species. With decreasing temperatures to 150 °C, natrolite becomes stable at the expense of nepheline at the lower log $a_{SiO_{2,aq}}$ limit of the analcime stability field. At low-temperature conditions (50 °C), natrolite is the dominant zeolite species, whereas the a_{H_2O} limit for natrolite stability decreases (Fig. 8). However, the textural relation indicates unambiguously that analcime is formed after natrolite. This indicates that the change from natrolite to analcime is either caused by an increase in temperature, or by an increase in SiO_2 activity (Fig. 8). An increase in temperature is implausible in the observed geological context. Alternatively, an increase of SiO_2 activity is achieved by the total breakdown of wollastonite, in contrast to the Fohberg phonolite, releasing SiO_2 to the fluid phase and Ca is trapped in calcite. However, the appearance of analcime is not pervasive and therefore the increase in SiO_2 activity seems to be more a local affect.

The cooling sequence natrolite-analcime is also known from other alkaline complexes, e.g., Mont St. Hilaire, Canada (Schilling et al. 2011) or Norra Kärr, Sweden (Atanasova et al. 2017), whereas in the Sushina Hill syenite, India (Chakrabarty et al. 2016), analcime formed at higher temperatures than associated natrolite.

IMPLICATIONS

Minerals of the zeolite group form the major secondary replacement products in holocrystalline, subvolcanic phonolites of the KVC. Zeolites are formed by the strongly selective decay of primary feldspathoid minerals, that is evident from pseudomorphic replacement textures and that is also known from other sites, e.g., from Tamazeght, Morocco, where gonnardite grows at the expense of nepheline, sodalite, and cancrinite due to late-stage reaction with meteoric waters (Salvi et al. 2000; Schilling et al. 2009), from Mont St. Hilaire, Canada, where natrolite and analcime grow along cracks and progressively replace sodalite (Schilling et al. 2011), and from the Sushina Hill Complex, India, where nepheline, sodalite (and albite) decompose to natrolite and analcime (Chakrabarty et al. 2016).

Several controlling factors are needed to "zeolitize" such rocks, which include favorable protolith mineralogy (e.g., feldspathoid minerals), the presence of a hydrothermal fluid with a promoting chemical composition (e.g., elevated pH), fluid accessibility to the rock (e.g., porosity, fracturing), and a *P-T* environment that stabilizes zeolite minerals. As a consequence, the geological setting is an important feature and may explain if an alkaline intrusive rock remains unaltered, or becomes partially or fully zeolitized. Weisenberger et al. (2014) have shown that fluid supply from the surrounding sedimentary rock sequence is an important factor for the intense and pervasive zeolite formation in the Fohberg phonolite. It is presumed that a local hydrothermal system was established, driven by the residual heat of the cooling intrusion, and mineral decomposition led to in situ or local replacement by zeolites, both in the rock matrix and in fissures. The same genetic model is applicable to the Endhalden phonolite, which is emplaced in the same geologic setting of the eastern KVC. The major difference between these two and the Kirchberg phonolite in the western KVC is found in the nature of the country rock. It is a water-bearing sedimentary sequence in the eastern localities, probably below the paleo-groundwater table, and a subaerial pyroclastic unit in the western locality (Kirchberg), which was probably relatively dry due to its high porosity and the higher topographic position in the volcanic edifice (Fig. 6).

In a general view, two temporal scenarios are capable of leading to the zeolitization of such intrusive rocks. (1) Zeolite formation in a continuously cooling regime, i.e., in the postmagmatic subsolidus stage after rock emplacement, which is characterized by the devel-

opment of a hydrothermal system. (2) Zeolite formation temporally unrelated to rock intrusion due to re-heating and re-emerging fluid activity, e.g., mineral formation in the waning stage of postdating regional metamorphism of an alkaline intrusive rock. Examples include Norra Kärr, Sweden (Atanasova et al. 2017) and Sushina Hill, India (Chakrabarty et al. 2016). Scenario 1 is the likely scenario for zeolitization of all KVC phonolites, which show no evidence of re-heating and reactivation of hydrothermal activity.

It is a noteworthy observation that these low-temperature secondary replacement reactions are capable of generating zeolite deposits of economic interest. In the example shown in this study, grades (total amount of zeolites, Supplemental[1] Table S1) of approximately 45% are achieved by total decomposition of igneous minerals mentioned above. Although not of such high grade as deposits formed by the crystallization of glass shards in uniform vitreous pyroclastic rocks, zeolite deposits in subvolcanic to plutonic SiO_2-deficient alkaline rocks are nevertheless suitable for several technical applications and should be considered as potentially valuable lithologies.

Despite their use as cation exchangers, natural zeolites show various other technical applications. One application is the production of blended cements, where zeolites serve as supplementary cementitious material (SCM) due to their pozzolanic reactivity (Snellings et al. 2012). The use of SCM becomes increasingly important as it reduces the need of ordinary Portland cement (OPC), and blended cements with a lower clinker ratio and higher SCM contents are commonly produced worldwide, instead of OPC. Therefore, because SCM has the potential to substitute for a certain amount of OPC, it accounts for a significant reduction of the CO_2 released during cement production, which is the third-largest source of anthropogenic CO_2 emissions (Andrew 2018).

Previous studies have shown that the pozzolanic reactivity of a rock used as SCM depends on various controlling factors, including the specific mineralogical phase assemblage of the rock, the grain sizes of the reactive phases as well as their behavior during industrial processing, e.g., grinding and thermal treatment. The combination of these factors complicates the comparison of different occurrences and the prediction of the reactivity (Mertens et al. 2009; Snellings et al. 2010a, 2010b; Özen et al. 2016). It is evident that each KVC phonolite, but also each occurrence worldwide, has to be evaluated independently for its potential use as SCM when the general mineralogical characteristics are promising.

Acknowledgments

We are grateful to Hans G. Hauri KG Mineralstoffwerke, Bötzingen, Germany, for access to the active Fohberg quarry and the Endhalden area, and for technical support. We acknowledge helpful discussions with O. Clemens, Darmstadt, about the quantitative X-ray analyses. We thank Linda Campbell and an anonymous reviewer for their detailed and constructive comments. Finally, we are grateful to the guest editor of the special collection on "Microporous Materials: Crystal-Chemistry, Properties And Utilizations," G.D. Gatta, Milan, for the editorial handling of our manuscript. This paper is dedicated to our friend and graduate supervisor (S.S., T.B.W.) Rune S. Selbekk (1967–2017), who introduced us to the science of zeolites and inspired us in our further profession.

References cited

Al Dwairi, R.A., Ibrahim, K.M., and Khoury, H.N. (2014) Potential use of faujasite-phillipsite and phillipsite-chabazite tuff in purification of treated effluent from domestic wastewater treatment plants. Environmental Earth Sciences, 71, 5071–5078.

Albrecht, A. (1981) Mineralogische Untersuchungen des Phonoliths vom Fohberg, Kaiserstuhl, mit besonderer Berücksichtigung der mafischen und akzessorischen Minerale. Diploma thesis, 146 p. Albert-Ludwigs-Universtity Freiburg.

Andrew, R.M. (2018) Global CO_2 emissions from cement production. Earth System Science Data, 10, 195–217.

Atanasova, P., Marks, M.A.W., Heinig, T., Krause, J., Gutzmer, J., and Markl, G. (2017) Distinguishing magmatic and metamorphic processes in peralkaline rocks of the Norra Kärr Complex (southern Sweden) using textural and compositional variations of clinopyroxene and eudialyte-group minerals. Journal of Petrology, 58, 361–384.

Baerlocher, C., McCusker, L.B., and Olson, D.H. (2007) Atlas of Zeolite Framework Types, 398 p. Elsevier.

Baranyi, I., Lippolt, H.J., and Todt, W. (1976) Kalium-Argon-Altersbestimmungen an tertiären Vulkaniten des Oberrheingraben-Gebiets II. Die Alterstraverse vom Hegau nach Lothringen. Oberrheinische Geologische Abhandlungen, 25, 41–62.

Barth-Wirsching, U., and Höller, H. (1989) Experimental studies on zeolite formation conditions. European Journal of Mineralogy, 1, 489–506.

Bernhard, F., and Barth-Wirsching, U. (2002) Zeolitization of a phonolitic ash flow by groundwater in the Laacher See volcanic area, Eifel, Germany. Clays and Clay Minerals, 50, 710–725.

Braunger, S., Marks, M.A.W., Walter, B.F., Neubauer, R., Reich, R., Wenzel, T., Parsapoor, A., and Markl, G. (2018) The petrology of the Kaiserstuhl Volcanic Complex, SW Germany: the importance of metasomatized and oxidized lithospheric mantle for carbonatite generation. Journal of Petrology, 59, 1731–1762.

Cappelletti, P., Petrosino, P., de Gennaro, M., Colella, A., Graziano, S.F., D'Amore, M., Mercurio, M., Cerri, G., de Gennaro, R., Rapisardo, G., and Langella, A. (2015) The "Tufo Giallo della Via Tiberina" (Sabatini Volcanic District, Central Italy): a complex system of lithification in a pyroclastic current deposit. Mineralogy and Petrology, 109, 85–101.

Chakrabarty, A., Mitchell, R., Ren, M., Saha, P., Pal, S., Pruseth, K., and Sen, A. (2016) Magmatic, hydrothermal and subsolidus evolution of the agpaitic nepheline syenites of the Sushina Hill Complex, India: implications for the metamorphism of peralkaline syenites. Mineralogical Magazine, 80, 1161–1193.

Cheary, R.W., and Coelho, A. (1992) A fundamental parameters approach to X-ray line-profile fitting. Journal of Applied Crystallography, 25, 109–121.

Çiftçi, E., Hogan, J.P., Kolayli, H., and Çadirli, E. (2008) Natrolitite, an unusual rock—occurrence and petrographic and geochemical characteristics (eastern Turkey). Clays and Clay Minerals, 56, 207–221.

Cochemé, J.J., Lassauvagerie, A.C., Gonzalez-Sandoval, J., Perez-Segura, E., and Münch, P. (1996) Characterisation and potential economic interest of authigenic zeolites in continental sediments from NW Mexico. Mineralium Deposita, 31, 482–491.

Coombs, D.S., Alberti, A., Artioli, A., Armbruster, T., Colella, C., Galli, E., Grice, J.D., Liebau, F., Mandarino, J.A., Minato, H., and others. (1997) Recommended nomenclature for zeolite minerals: report of the subcommittee on zeolites of the international mineralogical association, commission on new minerals and mineral names. Canadian Mineralogist, 35, 1571–1606.

Czygan, W. (1973) Götzenit, ein komplexes Ti-Zr-Silikat aus dem Kaiserstuhl. Berichte der naturforschenden Gesellschaft zu Freiburg i.Br., 63, 5–12.

——— (1977) Petrographie und Geochemie der Foidsyenit-Einschlüsse im Phonolith von Niederrotweil im Kaiserstuhl. Berichte der naturforschenden Gesellschaft zu Freiburg i.Br., 67, 41–52.

Deer, W.A., Howie, R.A., Wise. W.S., and Zussman, J. (2004) Framework silicates:silica minerals, feldspathoids and the zeolites. The Geological Society of London, London.

de'Gennaro, M., and Langella, A. (1996) Italian zeolitized rocks of technological interest. Mineralium Deposita, 31, 452–472.

de'Gennaro, M., Cappelletti, P., Langella, A., Perrotta, A., and Scarpati, C. (2000) Genesis of zeolites in the Neapolitan Yellow Tuff: geological, volcanological and mineralogical evidence. Contributions to Mineralogy and Petrology, 139, 17–35.

Eggleton, R.A., and Keller, J. (1982) The palagonitization of limburgitic glass—a TEM study. Neues Jahrbuch für Mineralogie, Monatsheft, 321–336.

Faccini, B., Di Giuseppe, D., Malferrari, D., Coltorti, M., Abbondanzi, F., Campisi, T., Laurora, A., and Passaglia, E. (2015) Ammonium-exchanged zeolitite preparation for agricultural uses: from laboratory tests to large-scale application in ZeoLIFE project prototype. Periodico di Mineralogia, 84, 303–321.

Harada, K., and Nagashima, K. (1972) New data on the analcime-wairakite series. American Mineralogist, 57, 924–931.

Hay, R.L., and Sheppard, R.A. (2001) Occurrence of zeolites in sedimentary rocks: An Overview. Reviews in Mineralogy and Geochemistry, 45, 217–234.

Helgeson, H.C., Delany, J.M., Nesbitt, H.W., and Bird, D.K. (1978) Summary and critique of the thermodynamic properties of rock-forming minerals. American Journal of Science, 278-A, 1–229.

Ibrahim, K.M. (2004) Mineralogy and chemistry of natrolite from Jordan. Clay Minerals, 39, 47–55.

Ibrahim, K.M., and Hall, A. (1996) The authigenic zeolites of the Aritayn volcanoclastic formation, north-east Jordan. Mineralium Deposita, 31, 514–522.

Ibrahim, K.M., Khoury, H.N., and Tuffaha, R. (2016) Mo and Ni removal from drinking water using zeolitic tuff from Jordan. Minerals, 6, 1–13.

Izzo, F., Grifa, C., Germinario, C., Mercurio, M., De Bonis, A., Tomay, L., and Langella, A. (2018) Production technology of mortar-based building materials from the Arch of Trajan and the Roman Theatre in Benevento, Italy. The European Physical Journal Plus, 133, 363.

Jackson, M.D., Mulcahy, S.R., Chen, H., Li, Y., Li, Q., Cappelletti, P., and Wenk, H.R. (2017) Phillipsite and Al-tobermorite mineral cements produced through low-temperature water-rock reactions in Roman marine concrete. American Mineralogist, 102, 1435–1450.

Johnson, J.W., Oelkers, E.H., and Helgeson, H.C. (1992) SUPCRT92: A software package for calculating the standard molal thermodynamic properties of minerals, gases, aqueous species, and reactions from 1 to 5000 bar and 0 to 1000°C. Computers and Geosciences, 18, 899–947.
Kalló, D. (2001) Applications of natural zeolites in water and wastewater treatment. Reviews in Mineralogy and Geochemistry, 45, 519–550.
Kassautzki, M. (1983) Phonolith als puzzolanischer Zumahlstoff in der Zementindustrie. Zement-Kalk-Gips International, 36, 688–692.
Keller, J. (1964) Zur Vulkanologie des Burkheim-Sponeck Gebietes im westlichen Kaiserstuhl. Berichte der naturforschenden Gesellschaft zu Freiburg i. Br., 54, 107–130.
——— (2001) Kaiserstuhl alkaline rock-carbonatitic complex—Excursion notes. ESF Carbonatite Workshop, Breisach.
Keller, J., Sigmund, J., and Müller-Sigmund, H. (1997) Mantle xenoliths in Rhinegraben volcanics from the Black Forest-Vosges Dome. Terra Nova, 9, Supplement, 1, 56.
Kónya, P., and Szakáll, S. (2011) Occurrence, composition and paragenesis of the zeolites and associated minerals in the alkaline basalt of a maar-type volcano at Haláp Hill, Balaton Highland, Hungary. Mineralogical Magazine, 75, 2869–2885.
Kousehlar, M., Weisenberger, T.B., Tutti, F., and Mirnejad, H. (2012) Fluid control on low-temperature mineral formation in volcanic rocks of Kahrizak, Iran. Geofluids, 12, 295–311.
Kraml, M., Pik, R., Rahn, M., Selbekk, R.S., Carignan, J., and Keller, J. (2006) A new multi-mineral age reference material for $^{40}Ar/^{39}Ar$, (U/Th)/He and fission track dating methods: The Limberg t3 tuff. Geostandards and Geoanalytical Research, 30, 73–86.
Langella, A., Bish, D.L., Cappelletti, P., Cerri, G., Colella, A., de'Gennaro, R., Graziano, S.F., Perrotta, A., Scarpati, C., and de'Gennaro, M. (2013) New insights into the mineralogical facies distribution of Campanian Ignimbrite, a relevant Italian industrial material. Applied Clay Science, 72, 55–73.
Leggo, P.J., and Ledésert, B. (2001) Use of organo-zeolitic fertilizer to sustain plant growth and stabilize metallurgical and mine-waste sites. Mineralogical Magazine, 65, 563–570.
Leggo, P.J., Ledésert, B., and Day, J. (2010) Organo-zeolitic treatment of mine waste to enhance the growth of vegetation. European Journal of Mineralogy, 22, 813–822.
Loewenstein, W. (1954) The distribution of aluminum in the tetrahedra of silicates and aluminates. American Mineralogist, 39, 92–96.
Madsen, I.C., and Scarlett, N.V.Y. (2008) Quantitative phase analysis. In R.E. Dinnebier and S.J.L. Billinge, Eds., Powder diffraction: theory and practice, p. 298–331. RSC Publishing, Cambridge, U.K.
Marzi, E. (1983) Die Mineralien des Fohbergs bei Bötzingen (Oberschaffhausen) im Kaiserstuhl. Der Aufschluss, 34, 205–214.
Marzi, E., and Spürgin, S. (2017) Neufund im klassischen Vulkangebiet—Merlinoit aus dem Kaiserstuhl. Lapis, 5, 12–23.
Mercurio, M., Mercurio, V., de Gennaro, B., de Gennaro, M., Grifa, C., Langella, A., and Morra, V. (2010) Natural zeolites and white wines from Campania region (Southern Italy): a new contribution for solving some oenological problems. Periodico di Mineralogia, 79, 95–112.
Mercurio, M., Cappelletti, P., de Gennaro, B., de Gennaro, M., Bovera, F., Iannaccone, F., Grifa, C., Langella, A., Monetti, V., and Esposito, L. (2016) The effect of digestive activity of pig gastro-intestinal tract on zeolite-rich rocks: An in vitro study. Microporous and Mesoporous Materials, 225, 133–136.
Mercurio, M., Izzo, F., Langella, A., Grifa, C., Germinario, C., Daković, A., Aprea, P., Pasquino, R., Cappelletti, P., Graziano, F.S., and De Gennaro, B. (2018) Surface-modified phillipsite-rich tuff from the Campania region (southern Italy) as a promising drug carrier: An ibuprofen sodium salt trial. American Mineralogist, 103, 700–710.
Mertens, G., Snellings, R., Van Balen, K., Bicer-Simsir, B., Verlooy, P., and Elsen, J. (2009) Pozzolanic reactions of common natural zeolites with lime and parameters affecting their reactivity. Cement and Concrete Research, 39, 233–240.
Napia, C., Sinsiri, T., Jaturapitakkul, C., and Chindaprasirt, P. (2012) Leaching of heavy metals from solidified waste using portland cement and zeolite as a binder. Waste Management, 32, 1459–1467.
Neuhoff, P.S. (2000) Thermodynamic properties and parageneses of rock-forming zeolites. Ph.D. thesis, 240 p. Stanford University, California.
Neuhoff, P.S., Fridriksson, T., Arnorsson, S., and Bird, D.K. (1999) Porosity evolution and mineral paragenesis during low-grade metamorphism of basaltic lavas at Teigarhorn, eastern Iceland. American Journal of Science, 299, 467–501.
Neuhoff, P.S., Rogers, K.L., Stannius, L.S., Bird, D.K., and Pedersen, A.K. (2006) Regional very low-grade metamorphism of basaltic lavas, Disko-Nuussuaq region, West Greenland. Lithos, 92, 33–54.
Özen, S., Göncüoğlu, M.C., Liguori, B., de Gennaro, B., Cappelletti, P., Gatta, G.D., Iucolano, F., and Colella, C. (2016) A comprehensive evaluation of sedimentary zeolites from Turkey as pozzolanic addition of cement- and lime-based binders. Construction and Building Materials, 105, 46–61.
Passaglia, E. (1970) The crystal chemistry of chabazite. American Mineralogist, 55, 1278–1301.
Rodriguez-Navarro, C., Ruiz-Agudo, E., Luque, A., Rodriguez-Navarro, A.B., and Ortega-Huertas, M. (2009) Thermal decomposition of calcite: Mechanisms of formation and textural evolution of CaO nanocrystals. American Mineralogist, 94, 578–593.
Rogers, K.L., Neuhoff, P.S., Pedersen, A.K., and Bird, D.K. (2006) CO_2 metasomatism in a basalt-hosted petroleum reservoir, Nuussuaq, West Greenland. Lithos, 92, 55–82.
Salvi, S., Fontan, F., Monchoux, P., Williams-Jones, A.E., and Moine, B. (2000) Hydrothermal mobilization of high field strength elements in alkaline igneous systems: Evidence from the Tamazeght complex (Morocco). Economic Geology, 95, 559–576.
Schilling, J., Marks, M.A.W., Wenzel, T., and Markl, G. (2009) Reconstruction of magmatic to subsolidus processes in an agpaitic system using eudialyte textures and composition: a case study from Tamazeght, Morocco. Canadian Mineralogist, 47, 351–365.
Schilling, J., Marks, M.A.W., Wenzel, T., Vennemann, T., Horváth, L., Tarassoff, P., Jacob, D.E., and Markl, G. (2011) The magmatic to hydrothermal evolution of the intrusive Mont Saint-Hilaire Complex: insights into the late-stage evolution of peralkaline rocks. Journal of Petrology, 52, 2147–2185.
Snellings, R., Mertens, G., Gasharova, B., Garbev, K., and Elsen, J. (2010a) The pozzolanic reaction between clinoptilolite and portlandite: a time and spatially resolved IR study. European Journal of Mineralogy, 22, 767–777.
Snellings, R., Mertens, G., and Elsen, J. (2010b) Calorimetric evolution of the early pozzolanic reaction of natural zeolites. Journal of Thermal Analysis and Calorimetry, 101, 97–105.
Snellings, R., Mertens, G., and Elsen, J. (2012) Supplementary cementitious materials. Reviews in Mineralogy and Geochemistry, 74, 211–278.
Spürgin, S., Weisenberger, T., and Hörth, J. (2008) Das Leucitophyrvorkommen vom Strümpfekopf im Kaiserstuhl—eine historische und mineralogische Betrachtung. Berichte der naturforschenden Gesellschaft zu Freiburg i.Br., 98, 221–244.
Spürgin, S., Weisenberger, T., Rosing-Schow, N., and Vasilopoulos, M. (2014) Phonolite-hosted zeolite deposits in the Kaiserstuhl Volcanic Complex, Germany. Zeolites 2014 Book of Abstracts, Belgrade, 221–222.
Tschernich, R.W. (1992) Zeolites of the World, 563 p. Geoscience Press, Phoenix.
van Reeuwijk, L.P. (1972) High-temperature phases of zeolites of the natrolite group. American Mineralogist, 57, 499–510.
Wedepohl, K.H., Gohn, E., and Hartmann, G. (1994) Cenozoic alkali basaltic magmas of western Germany and their products of differentiation. Contributions to Mineralogy and Petrology, 115, 253–278.
Weisenberger, T., and Selbekk, R.S. (2009) Multi-stage zeolite facies mineralization in the Hvalfjördur area, Iceland. International Journal of Earth Sciences, 98, 985–999.
Weisenberger, T., and Spürgin, S. (2009) Zeolites in alkaline rocks of the Kaiserstuhl Volcanic Complex—new microprobe investigation and their relationship to the host rock. Geologica Belgica, 12, 75–91.
Weisenberger, T.B., Spürgin, S., and Lahaye, Y. (2014) Hydrothermal alteration and zeolitization of the Fohberg phonolite, Kaiserstuhl Volcanic Complex, Germany. International Journal of Earth Sciences, 103, 2273–2300.
Whitney, D.L., and Evans, B.W. (2010) Abbreviations for names of rock-forming minerals. American Mineralogist, 95, 185–187.
Wilson, M., and Downes, H. (1991) Tertiary-Quaternary extension-related alkaline magmatism in western and central Europe. Journal of Petrology, 32, 811–849.
Wimmenauer, W. (1962) Beiträge zur Petrographie des Kaiserstuhls. Teil IV: Die Gesteine der phonolitischen Familie. Teil V: Die subvulkanischen Breccien. Neues Jahrbuch für Mineralogie Abhandlungen, 98, 367–415.
——— (1974) The alkaline province of central Europe and France. In H. Sorensen, Ed., The Alkaline Rocks, p. 286–291. Wiley.
——— (2003) Geologische Karte von Baden-Württemberg 1:25 000, Kaiserstuhl. Landesamt für Geologie, Rohstoffe und Bergbau Baden-Württemberg, Freiburg.
——— (2010) Kalkadern in vulkanischen und Sedimentgesteinen des Kaiserstuhls. Mitteilungen des badischen Landesvereins für Naturkunde und Naturschutz, 21, 49–67.

Manuscript received September 30, 2018
Manuscript accepted February 11, 2019
Manuscript handled by G. Diego Gatta

Endnote:

[1]Deposit item AM-19-56831, Supplemental Figures and Tables. Deposit items are free to all readers and found on the MSA website, via the specific issue's Table of Contents (go to http://www.minsocam.org/MSA/AmMin/TOC/2019May2019_data/May2019_data.html).